combined inhibitory effect against both BMP and Wnt canonical signals via LRP6 by direct binding (Nakamura *et al.* 2007).

The case of CCN6 depicts the general property of the CCN family of genes. Basic molecular interactions or signal transduction seemed to be well conserved among animal species, but the phenotype of genetic mutations is rather different. This may be because the emphasis of CCN family signal usage is different from species to species. CCN may be still evolving to keep pace with vertebrate evolution. It may be that vertebrates use CCN to evolve their own method of organogenesis.

CCN and relative families

Each domain of CCN is shared with a large number of genes, but the combination and order of the four modules is specific to the CCN family. However, partial homology with the CCN family is found in several gene families (Fig. 8). In the N-terminal domain (IGFBP~), the IGFBP and Tsg families share homology with CCN (Hwa *et al.* 1999). For the C-terminal domain (CT), DAN, Sost/Wise, and Slit families are related (Ellies *et al.* 2006). Among these families, CCN and Sost/Wise families do not have equivalent genes in invertebrates, which implies that these two families evolved with the emergence of vertebrates. Most members of the IGFP family are vertebrate-specific, but only IGFBP 7 has an equivalent in *Drosophila* (Imp-L2), which counteracts insulin signaling and is essential for starvation resistance (Honegger *et al.* 2008).

The N-terminal homologous domains of CCN, IGFBP and Tsg are consistent in size, at about 80 amino acid residues. The similarity of the three families depends on the conserved cysteine residues, which constitute a conserved local motif (xC-x-CC-x(2)-C-x(3)-LG), namely GCGCC-x(2)-C. The GCGCC-x(2)-C motif is a putative interacting domain with IGFs (Finelli *et al.* 1994).

Tsg was identified in *Drosophila* as one of seven zygotic dorso-ventral polarity genes that specify the cell fate antagonizing *decapentaplegic* (*DPP*) gene (Mason *et al.* 1994). Dorso-ventral patterning in vertebrates is also regulated by a gradient of BMP activity, and vertebrate Tsg was identified as a BMP-binding protein that acts as an antagonist, a novel member of the BMP signaling pathway like chordin or noggin (Oelgeschlager *et al.* 2000). From protein database analyses, these three gene families share weak similarity except for the IGFBP domain. Grotendorst *et al.* have argued that *CCN* and *IGFBP* are two distinct families and that the CCN family should not be considered as a part of the *IGFBP* family (Grotendorst *et al.* 2000). However, these families have also been grouped together in the TIC superfamily (Tsg, IGFBP, and CCN) (Vilmos *et al.* 2001).

The C-terminal domain of CCN is homologous to other gene families. From 2001 to 2003, genes homologous to the CCN C-terminal domain were reported. *Sclerostosis* was identified through homozygosity mapping followed by positional gene cloning from patients that showed an autosomal recessive sclerosing bone dysplasia characterized by progressive skeletal overgrowth (Brunkow *et al.* 2001). Independent mutations were found in this novel gene, whose product was termed Sclerostin. SOST contains a cystine knot motif (residues 80–167) that is similar to the CT domain of CCN. The main function of SOST is antagonistic activity against BMP (Kusu *et al.* 2003), but SOST may also antagonistically interact with LRP5 in bone mass regulation (Li *et al.* 2005; Ellies *et al.* 2006).

Itasaki *et al.* have isolated the novel secreted molecule Wise, by functional screening for activities that alter the anteroposterior character of neuralized *Xenopus* animal caps (Itasaki *et al.* 2003). *Wise* encodes a secreted protein that has similarity with CCN in the C-terminal domain. Phenotypes arising from ectopic expression or depletion of Wise negatively correlate to Wnt signaling. Wise has been demonstrated to interact with LRP6 to retain it in the endoplasmic reticulum, which attenuates Wnt signaling (Guidato & Itasaki 2007). Wise has two synonymous names in mammals: ectodin (mouse) and USAG-1 (rat) (Table 1). A secreted BMP antagonist, namely ectodin (ectodermal BMP inhibitor) was identified in mouse ectodermal tissues (Laurikkala *et al.* 2003). Recombinant ectodin protein produced in cultured cells inhibits the activity of BMP2, BMP4, BMP6, and BMP7. A knockout of ectodin causes abnormal tooth cusp development with hyperactivation of BMP signaling (Kassai *et al.* 2005). Also, a gene induced in the rat endometrium at the time of uterine receptivity/sensitization for the decidual cell reaction, known as *Uterine sensitization-associated gene-1* (*USAG-1*) (Simmons & Kennedy 2002), is an equivalent gene of ectodin and has been demonstrated to be a BMP antagonist (Yanagita *et al.* 2004). Contrary to the role of Wise in chicken, these mammalian equivalents principally act as BMP antagonists. These facts may indicate that the role of the Wise family differentially evolved depending on the vertebrate species.

The C-terminal domain of CCN also has high similarity to the Dan family, including *Dan*, *Cerberus*, *Gremlin*, and *Caronte*, which have been shown to act as BMP antagonists. In *Drosophila*, *Slit* has been shown to play a critical role in central nervous system midline formation. Itoh *et al.* (1998) cloned the *SLIT* gene, a human homolog of the *Drosophila Slit*. They also cloned two additional *Slit* homologs. The Slit gene family also shares weak homology with the CT domain of CCN. The effect of Slit is rather different from other relatives,

since Slit interacts with ROBO, a member of the neural cell adhesion molecule (NCAM) family in axonal guidance as a ligand (Liu *et al.* 2004). Other proteins interacting with Slit have not yet been conclusively found.

The molecular evolution of CCN is not yet clearly understood, but it seems to have evolved with its relative gene families in vertebrates (chordates). However, the bipolar similarities in the N-terminal and C-terminal domains with their relative gene families raise the question if CCN emergence is the result of genetic convergence or divergence. Recently, a chordin-like secreted molecule, *Tsukushi*, was identified from signal sequence trap screening using a chicken embryonic lens library (Ohta *et al.* 2004). This gene has very weak homology to CCN (VWC domain in CCN), and has the similar property of interacting with BMP, Notch (Delta and Jagged), and Wnt (LRP) signals. *Tsukushi* regulates various types of stem cells in the primitive streak, neural crest, and retina (Ohta *et al.* 2006; Ohta *et al.* 2008) like CCNs. R-spondin is relatively distant from CCN, but has a Wnt inhibitory effect in the same manner as Wise/Sost (Hendrickx & Leyns 2008). It may be possible that there still exist some unknown secreted factors in vertebrates that bind and regulate the principal developmental signals.

CCN and tumor malignancy

In this review, we have not discussed much about the role of CCNs in adult tissues, but a number of investigations indicate their implication in tumor malignancy. In the case of CCN3, it has been suggested that this CCN is positively correlated to malignant behavior (invasiveness, cell migration) of melanoma cells (Vallacchi *et al.* 2008), but another report demonstrated inverted results (Fukunaga-Kalabis *et al.* 2008). Vallacchi *et al.* studied clinical cases of melanomas demonstrating that highly metastatic cases showed relatively high expression of CCN3. They also demonstrated that melanoma cell lines transfected with CCN3 showed wide and rapid metastasis in distant organs as compared with non-transfected ones. Fukunaga-Kalabis *et al.* also studied clinical cases of melanomas from the aspect of skin invasion patterns and demonstrated aggressive invasion related to the low level expression of CCN3. They applied a skin graft experiment of melanoma cell lines transfected with CCN3 and demonstrated low invasiveness of transfected melanomas. Both reports confirmed that overexpression of CCN3 upregulates the cell adhesiveness of melanoma cells. Vallacchi *et al.* claim that upregulation of cell adhesiveness enhances the nesting of metastatizing cells in remote areas, while Fukunaga-Kalabis *et al.* argue that cell adhesiveness to the basement membrane proteins cause low invasion of melanoma cells. Their reports are consistent in that CCN3 exerts cell adhesive effects. Their differing conclusions might be because CCN3 biological effects may differ depending on the spatial situation of melanoma cells.

Conclusions

In brief, a number of reports have brought evidence that the CCN family of genes interacts with various extracellular matrix proteins, transmembrane proteins, growth factors, and cytokines. Particularly, its interaction with BMP, Wnt, and Notch, members of tool kit genes in development (Ryan & Baxevanis 2007; De Robertis 2008), is important. The phenotypes of CCN transgenic animals are mainly concerned with vasculo/angiogenesis and osteo/chondrogenesis, but it is various among animal species. Cell biological analysis *in vitro* demonstrates that these interactions are sometimes synergistic, but also sometimes antagonistic. However, CCN seems to help *in vivo* tissue construction, organizing the spatio-temporal activation/suppression of these genes. This type of fine-tuning may relate to the strong regeneration capacity of vertebrates. It is possible that deletion or mutation constructs of CCNs clearly depict the function of each domain. Further study will help not only in understanding the complicated nature of CCNs, but also give some idea for new drug development such as for regenerative therapy or anti-tumor progression.

Acknowledgements

We greatly appreciate the ardent reading and critical comments of Dr H. Nakamura about our manuscript. We also appreciate the unpublished information and the helpful discussion in the 5th International meeting of CCN family of genes. This work is supported by the Grant-in-Aid of the Japanese Society of the Promotion of Sciences (JSPS 20592135 for Ken-ichi Katsube), Japan.

References

Abreu, J. G., Ketpura, N. I., Reversade, B. & De Robertis, E. M. 2002. Connective-tissue growth factor (CTGF) modulates cell signalling by BMP and TGF-beta. *Nat. Cell Biol.* **4**, 599–604.

Babic, A. M., Chen, C. C. & Lau, L. F. 1999. Fisp12/mouse connective tissue growth factor mediates endothelial cell adhesion and migration through integrin alphavbeta3, promotes endothelial cell survival, and induces angiogenesis *in vivo*. *Mol. Cell. Biol.* **19**, 2958–2966.

Bradham, D. M., Igarashi, A., Potter, R. L. & Grotendorst, G. R. 1991. Connective tissue growth factor: a cysteine-rich mitogen secreted by human vascular endothelial cells is related to the SRC-induced immediate early gene product CEF-10. *J. Cell Biol.* **114**, 1285–1294.

Brigstock, D. R., Goldschmeding, R., Katsube, K. I., Lam, S. C., Lau, L. F., Lyons, K., Naus, C., Perbal, B., Riser, B., Takigawa,

M. & Yeger, H. 2003. Proposal for a unified CCN nomenclature. *Mol. Pathol.* **56**, 127–128.

Brunkow, M. E., Gardner, J. C., Van Ness, J., Paeper, B. W., Kovacevich, B. R., Proll, S., Skonier, J. E., Zhao, L., Sabo, P. J., Fu, Y., Alisch, R. S., Gillett, L., Colbert, T., Tacconi, P., Galas, D., Hamersma, H., Beighton, P. & Mulligan, J. 2001. Bone dysplasia sclerosteosis results from loss of the SOST gene product, a novel cystine knot-containing protein. *Am. J. Hum. Genet.* **68**, 577–589.

Calhabeu, F., Lafont, J., L. E. Dreau, G., Laurent, M., Kazazian, C., Schaeffer, L., Martinerie, C. & Dubois, C. 2006. NOV/CCN3 impairs muscle cell commitment and differentiation. *Exp. Cell. Res.* **312**, 1876–1889.

Carmeliet, P., Ferreira, V., Breier, G., Pollefeyt, S., Kieckens, L., Gertsenstein, M., Fahrig, M., Vandenhoeck, A., Harpal, K., Eberhardt, C., Declercq, C., Pawling, J., Moons, L., Collen, D., Risau, W. & Nagy, A. 1996. Abnormal blood vessel development and lethality in embryos lacking a single VEGF allele. *Nature* **380**, 435–439.

Chen, N., Leu, S. J., Todorovic, V., Lam, S. C. & Lau, L. F. 2004. Identification of a novel integrin alphavbeta3 binding site in CCN1 (CYR61) critical for pro-angiogenic activities in vascular endothelial cells. *J. Biol. Chem.* **279**, 44166–44176.

Chen, Y., Ni, H., Ma, X. H., Hu, S. J., Luan, L. M., Ren, G., Zhao, Y. C., Li, S. J., Diao, H. L., Xu, X., Zhao, Z. A. & Yang, Z. M. 2006. Global analysis of differential luminal epithelial gene expression at mouse implantation sites. *J. Mol. Endocrinol.* **37**, 147–161.

Chiou, M. J., Chao, T. T., Wu, J. L., Kuo, C. M. & Chen, J. Y. 2006. The physiological role of CTGF/CCN2 in zebrafish notochord development and biological analysis of the proximal promoter region. *Biochem. Biophys. Res. Commun.* **349**, 750–758.

Crean, J. K., Furlong, F., Mitchell, D., McArdle, E., Godson, C. & Martin, F. 2006. Connective tissue growth factor/CCN2 stimulates actin disassembly through Akt/protein kinase B-mediated phosphorylation and cytoplasmic translocation of p27(Kip-1). *FASEB J.* **20**, 1712–1714.

De Robertis, E. M. 2008. Evo-devo: variations on ancestral themes. *Cell* **132**, 185–195.

Ehl, S., Uhl, M., Berner, R., Bonafe, L., Superti-Furga, A. & Kirchhoff, A. 2004. Clinical, radiographic, and genetic diagnosis of progressive pseudorheumatoid dysplasia in a patient with severe polyarthropathy. *Rheumatol. Int.* **24**, 53–56.

Ellies, D. L., Viviano, B., McCarthy, J., Rey, J. P., Itasaki, N., Saunders, S. & Krumlauf, R. 2006. Bone density ligand, Sclerostin, directly interacts with LRP5 but not LRP5G171V to modulate Wnt activity. *J. Bone Miner. Res.* **21**, 1738–1749.

Finelli, A. L., Bossie, C. A., Xie, T. & Padgett, R. W. 1994. Mutational analysis of the Drosophila tolloid gene, a human BMP-1 homolog. *Development* **120**, 861–870.

Fischer, A., Steidl, C., Wagner, T. U., Lang, E., Jakob, P. M., Friedl, P., Knobeloch, K. P. & Gessler, M. 2007. Combined loss of Hey1 and HeyL causes congenital heart defects because of impaired epithelial to mesenchymal transition. *Circ. Res.* **100**, 856–863.

Fukunaga-Kalabis, M., Martinez, G., Telson, S. M., Liu, Z. J., Balint, K., Juhasz, I., Elder, D. E., Perbal, B. & Herlyn, M. 2008. Downregulation of CCN3 expression as a potential mechanism for melanoma progression. *Oncogene* **27**, 2552–2560.

Gao, R. & Brigstock, D. R. 2006. A novel integrin alpha5beta1 binding domain in module 4 of connective tissue growth factor (CCN2/CTGF) promotes adhesion and migration of activated pancreatic stellate cells. *Gut* **55**, 856–862.

Gasperowicz, M. & Otto, F. 2008. The notch signalling pathway in the development of the mouse placenta. *Placenta* **29**, 651–659.

Grotendorst, G. R., Lau, L. F. & Perbal, B. 2000. CCN proteins are distinct from and should not be considered members of the insulin-like growth factor-binding protein superfamily. *Endocrinology* **141**, 2254–2256.

Guidato, S. & Itasaki, N. 2007. Wise retained in the endoplasmic reticulum inhibits Wnt signaling by reducing cell surface LRP6. *Dev. Biol.* **310**, 250–263.

Hashimoto, G., Inoki, I., Fujii, Y., Aoki, T., Ikeda, E. & Okada, Y. 2002. Matrix metalloproteinases cleave connective tissue growth factor and reactivate angiogenic activity of vascular endothelial growth factor 165. *J. Biol. Chem.* **277**, 36288–36295.

Hendrickx, M. & Leyns, L. 2008. Non-conventional Frizzled ligands and Wnt receptors. *Dev. Growth Differ.* **50**, 229–243.

Honegger, B., Galic, M., Kohler, K., Wittwer, F., Brogiolo, W., Hafen, E. & Stocker, H. 2008. Imp-L2, a putative homolog of vertebrate IGF-binding protein 7, counteracts insulin signaling in Drosophila and is essential for starvation resistance. *J. Biol.* **7**, 10.

Hoshijima, M., Hattori, T., Inoue, M., Araki, D., Hanagata, H., Miyauchi, A. & Takigawa, M. 2006. CT domain of CCN2/CTGF directly interacts with fibronectin and enhances cell adhesion of chondrocytes through integrin alpha5beta1. *FEBS Lett.* **580**, 1376–1382.

Hurvitz, J. R., Suwairi, W. M., Van Hul, W., El-Shanti, H., Superti-Furga, A., Roudier, J., Holderbaum, D., Pauli, R. M., Herd, J. K., Van Hul, E. V., Rezai-Delui, H., Legius, E., L. E. Merrer, M., Al-Alami, J., Bahabri, S. A. & Warman, M. L. 1999. Mutations in the CCN gene family member WISP3 cause progressive pseudorheumatoid dysplasia. *Nat. Genet.* **23**, 94–98.

Hwa, V., Oh, Y. & Rosenfeld, R. G. 1999. The insulin-like growth factor-binding protein (IGFBP) superfamily. *Endocr. Rev.* **20**, 761–787.

Inoki, I., Shiomi, T., Hashimoto, G., Enomoto, H., Nakamura, H., Makino, K., Ikeda, E., Takata, S., Kobayashi, K. & Okada, Y. 2002. Connective tissue growth factor binds vascular endothelial growth factor (VEGF) and inhibits VEGF-induced angiogenesis. *FASEB J.* **16**, 219–221.

Itasaki, N., Jones, C. M., Mercurio, S., Rowe, A., Domingos, P. M., Smith, J. C. & Krumlauf, R. 2003. Wise, a context-dependent activator and inhibitor of Wnt signalling. *Development* **130**, 4295–4305.

Itoh, A., Miyabayashi, T., Ohno, M. & Sakano, S. 1998. Cloning and expressions of three mammalian homologues of Drosophila slit suggest possible roles for slit in the formation and maintenance of the nervous system. *Mol. Brain. Res.* **62**, 175–186.

Ivkovic, S., Yoon, B. S., Popoff, S. N., Safadi, F. F., Libuda, D. E., Stephenson, R. C., Daluiski, A. & Lyons, K. M. 2003. Connective tissue growth factor coordinates chondrogenesis and angiogenesis during skeletal development. *Development* **130**, 2779–2791.

Kassai, Y., Munne, P., Hotta, Y., Penttila, E., Kavanagh, K., Ohbayashi, N., Takada, S., Thesleff, I., Jernvall, J. & Itoh, N. 2005. Regulation of mammalian tooth cusp patterning by ectodin. *Science* **309**, 2067–2070.

Katsube, K., Chuai, M. L., Liu, Y. C., Kabasawa, Y., Takagi, M., Perbal, B. & Sakamoto, K. 2001. The expression of chicken NOV, a member of the CCN gene family, in early stage development. *Brain Res. Gene Expr. Patterns* **1**, 61–65.

Katsuki, Y., Sakamoto, K., Minamizato, T., Makino, H., Umezawa, A., Ikeda, M. A., Perbal, B., Amagasa, T., Yamaguchi, A. & Katsube, K. 2008. Inhibitory effect of CT domain of CCN3/NOV on proliferation and differentiation of osteogenic

mesenchymal stem cells, Kusa-A1. *Biochem. Biophys. Res. Commun.* **368**, 808–814.

Kusu, N., Laurikkala, J., Imanishi, M., Usui, H., Konishi, M., Miyake, A., Thesleff, I. & Itoh, N. 2003. Sclerostin is a novel secreted osteoclast-derived bone morphogenetic protein antagonist with unique ligand specificity. *J. Biol. Chem.* **278**, 24113–24117.

Kutz, W. E., Gong, Y. & Warman, M. L. 2005. WISP3, the gene responsible for the human skeletal disease progressive pseudorheumatoid dysplasia, is not essential for skeletal function in mice. *Mol. Cell. Biol.* **25**, 414–421.

Latinkic, B. V., Mercurio, S., Bennett, B., Hirst, E. M., Xu, Q., Lau, L. F., Mohun, T. J. & Smith, J. C. 2003. Xenopus Cyr61 regulates gastrulation movements and modulates Wnt signalling. *Development* **130**, 2429–2441.

Lau, L. F. & Nathans, D. 1987. Expression of a set of growth-related immediate early genes in BALB/c 3T3 cells: coordinate regulation with c-fos or c-myc. *Proc. Natl Acad. Sci. USA* **84**, 1182–1186.

Laurikkala, J., Kassai, Y., Pakkasjarvi, L., Thesleff, I. & Itoh, N. 2003. Identification of a secreted BMP antagonist, ectodin, integrating BMP, FGF, and SHH signals from the tooth enamel knot. *Dev. Biol.* **264**, 91–105.

Leu, S. J., Liu, Y., Chen, N., Chen, C. C., Lam, S. C. & Lau, L. F. 2003. Identification of a novel integrin alpha 6 beta 1 binding site in the angiogenic inducer CCN1 (CYR61). *J. Biol. Chem.* **278**, 33801–33808.

Li, X., Zhang, Y., Kang, H., Liu, W., Liu, P., Zhang, J., Harris, S. E. & Wu, D. 2005. Sclerostin binds to LRP5/6 and antagonizes canonical Wnt signaling. *J. Biol. Chem.* **280**, 19883–19887.

Lin, C. G., Leu, S. J., Chen, N., Tebeau, C. M., Lin, S. X., Yeung, C. Y. & Lau, L. F. 2003. CCN3 (NOV) is a novel angiogenic regulator of the CCN protein family. *J. Biol. Chem.* **278**, 24200–24208.

Liu, Z., Patel, K., Schmidt, H., Andrews, W., Pini, A. & Sundaresan, V. 2004. Extracellular Ig domains 1 and 2 of Robo are important for ligand (Slit) binding. *Mol. Cell. Neurosci.* **26**, 232–240.

Marik, I., Marikova, O., Zemkova, D., Kuklik, M. & Kozlowski, K. 2004. Dominantly inherited progressive pseudorheumatoid dysplasia with hypoplastic toes. *Skeletal. Radiol.* **33**, 157–164.

Mason, E. D., Konrad, K. D., Webb, C. D. & Marsh, J. L. 1994. Dorsal midline fate in Drosophila embryos requires twisted gastrulation, a gene encoding a secreted protein related to human connective tissue growth factor. *Genes Dev.* **8**, 1489–1501.

Mercurio, S., Latinkic, B., Itasaki, N., Krumlauf, R. & Smith, J. C. 2004. Connective-tissue growth factor modulates WNT signalling and interacts with the WNT receptor complex. *Development* **131**, 2137–2147.

Minamizato, T., Sakamoto, K., Liu, T., Kokubo, H., Katsube, K., Perbal, B., Nakamura, S. & Yamaguchi, A. 2007. CCN3/NOV inhibits BMP-2-induced osteoblast differentiation by interacting with BMP and Notch signaling pathways. *Biochem. Biophys. Res. Commun.* **354**, 567–573.

Mo, F. E. & Lau, L. F. 2006. The matricellular protein CCN1 is essential for cardiac development. *Circ. Res.* **99**, 961–969.

Mo, F. E., Muntean, A. G., Chen, C. C., Stolz, D. B., Watkins, S. C. & Lau, L. F. 2002. CYR61 (CCN1) is essential for placental development and vascular integrity. *Mol. Cell. Biol.* **22**, 8709–8720.

Nakamura, Y., Weidinger, G., Liang, J. O., Aquilina-Beck, A., Tamai, K., Moon, R. T. & Warman, M. L. 2007. The CCN family member Wisp3, mutant in progressive pseudorheumatoid dysplasia, modulates BMP and Wnt signaling. *J. Clin. Invest.* **117**, 3075–3086.

Nakaya, Y., Sukowati, E. W., Wu, Y. & Sheng, G. 2008. RhoA and microtubule dynamics control cell-basement membrane interaction in EMT during gastrulation. *Nat. Cell Biol.* **10**, 765–775.

Nishida, T., Kawaki, H., Baxter, R. M., Deyoung, R. A., Takigawa, M. & Lyons, K. M. 2007. CCN2 (Connective Tissue Growth Factor) is essential for extracellular matrix production and integrin signaling in chondrocytes. *J. Cell Commun Signal* **1**, 45–58.

Oelgeschlager, M., Larrain, J., Geissert, D. & De Robertis, E. M. 2000. The evolutionarily conserved BMP-binding protein Twisted gastrulation promotes BMP signalling. *Nature* **405**, 757–763.

Ohta, K., Ito, A. & Tanaka, H. 2008. Neuronal stem/progenitor cells in the vertebrate eye. *Dev. Growth Differ.* **50**, 253–259.

Ohta, K., Kuriyama, S., Okafuji, T., Gejima, R., Ohnuma, S. & Tanaka, H. 2006. Tsukushi cooperates with VG1 to induce primitive streak and Hensen's node formation in the chick embryo. *Development* **133**, 3777–3786.

Ohta, K., Lupo, G., Kuriyama, S., Keynes, R., Holt, C. E., Harris, W. A., Tanaka, H. & Ohnuma, S. 2004. Tsukushi functions as an organizer inducer by inhibition of BMP activity in cooperation with chordin. *Dev. Cell* **7**, 347–358.

Ota, H., Katsube, K., Ogawa, J. & Yanagishita, M. 2007. Hypoxia/Notch signaling in primary culture of rat lymphatic endothelial cells. *FEBS Lett.* **581**, 5220–5226.

Parisi, M. S., Gazzerro, E., Rydziel, S. & Canalis, E. 2006. Expression and regulation of CCN genes in murine osteoblasts. *Bone* **38**, 671–677.

Pennica, D., Swanson, T. A., Welsh, J. W., Roy, M. A., Lawrence, D. A., Lee, J., Brush, J., Taneyhill, L. A., Deuel, B., Lew, M., Watanabe, C., Cohen, R. L., Melhem, M. F., Finley, G. G., Quirke, P., Goddard, A. D., Hillan, K. J., Gurney, A. L., Botstein, D. & Levine, A. J. 1998. WISP genes are members of the connective tissue growth factor family that are up-regulated in wnt-1-transformed cells and aberrantly expressed in human colon tumors. *Proc. Natl Acad. Sci. USA* **95**, 14717–14722.

Perbal, B. 2008. CCN3-mutant mice are distinct from CCN3-null mice. *J. Cell Commun. Signal.*

Perbal, B., Lipsick, J. S., Svoboda, J., Silva, R. F. & Baluda, M. A. 1985. Biologically active proviral clone of myeloblastosis-associated virus type 1: implications for the genesis of avian myeloblastosis virus. *J. Virol.* **56**, 240–244.

Perbal, B. & Takigawa, M. 2005. *CCN Proteins a New Family of Cell Growthad Differentiation Regulators*. Imperial College Press, London.

Pi, L., Ding, X., Jorgensen, M., Pan, J. J., Oh, S. H., Pintilie, D., Brown, A., Song, W. Y. & Petersen, B. E. 2008. Connective tissue growth factor with a novel fibronectin binding site promotes cell adhesion and migration during rat oval cell activation. *Hepatology* **47**, 996–1004.

Ryan, J. F. & Baxevanis, A. D. 2007. Hox, Wnt, and the evolution of the primary body axis: insights from the early-divergent phyla. *Biol. Direct* **2**, 37.

Rydziel, S., Stadmeyer, L., Zanotti, S., Durant, D., Smerdel-Ramoya, A. & Canalis, E. 2007. Nephroblastoma overexpressed (Nov) inhibits osteoblastogenesis and causes osteopenia. *J. Biol. Chem.* **282**, 19762–19772.

Sakamoto, K., Yamaguchi, S., Ando, R., Miyawaki, A., Kabasawa, Y., Takagi, M., Li, C. L., Perbal, B. & Katsube, K. 2002. The nephroblastoma overexpressed gene (NOV/ccn3) protein associates with Notch1 extracellular domain and inhibits myoblast differentiation via Notch signaling pathway. *J. Biol. Chem.* **277**, 29399–29405.

Segarini, P. R., Nesbitt, J. E., Li, D., Hays, L. G., Yates, J. R., 3rd &

Carmichael, D. F. 2001. The low density lipoprotein receptor-related protein/alpha2-macroglobulin receptor is a receptor for connective tissue growth factor. *J. Biol. Chem.* **276**, 40659–40667.

Simmons, D. G. & Kennedy, T. G. 2002. Uterine sensitization-associated gene-1: a novel gene induced within the rat endometrium at the time of uterine receptivity/sensitization for the decidual cell reaction. *Biol. Reprod.* **67**, 1638–1645.

Smerdel-Ramoya, A., Zanotti, S., Derogowski, V. & Canalis, E. 2008a. Connective tissue growth factor (CTGF) enhances osteoblastogenesis *in vitro*. *J Biol Chem*.

Smerdel-Ramoya, A., Zanotti, S., Stadmeyer, L., Durant, D. & Canalis, E. 2008b. Skeletal overexpression of connective tissue growth factor (ctgf) impairs bone formation and causes osteopenia. *Endocrinology*.

Suchting, S., Freitas, C., Le Noble, F., Benedito, R., Breant, C., Duarte, A. & Eichmann, A. 2007. The Notch ligand Delta-like 4 negatively regulates endothelial tip cell formation and vessel branching. *Proc. Natl Acad. Sci. USA* **104**, 3225–3230.

Tada, M. & Smith, J. C. 2000. Xwnt11 is a target of Xenopus Brachyury: regulation of gastrulation movements via Dishevelled, but not through the canonical Wnt pathway. *Development* **127**, 2227–2238.

Vallacchi, V., Daniotti, M., Ratti, F., Di Stasi, D., Deho, P., De Filippo, A., Tragni, G., Balsari, A., Carbone, A., Rivoltini, L., Parmiani, G., Lazar, N., Perbal, B. & Rodolfo, M. 2008. CCN3/nephroblastoma overexpressed matricellular protein regulates integrin expression, adhesion, and dissemination in melanoma. *Cancer Res.* **68**, 715–723.

Vilmos, P., Gaudenz, K., Hegedus, Z. & Marsh, J. L. 2001. The Twisted gastrulation family of proteins, together with the IGFBP and CCN families, comprise the TIC superfamily of cysteine rich secreted factors. *Mol. Pathol.* **54**, 317–323.

Watanabe, Y., Kokubo, H., Miyagawa-Tomita, S., Endo, M., Igarashi, K., Aisaki, K., Kanno, J. & Saga, Y. 2006. Activation of Notch1 signaling in cardiogenic mesoderm induces abnormal heart morphogenesis in mouse. *Development* **133**, 1625–1634.

Weinstein, B. M. & Lawson, N. D. 2002. Arteries, veins, Notch, and VEGF. *Cold Spring Harb. Symp. Quant. Biol.* **67**, 155–162.

Witze, E. S., Litman, E. S., Argast, G. M., Moon, R. T. & Ahn, N. G. 2008. Wnt5a control of cell polarity and directional movement by polarized redistribution of adhesion receptors. *Science* **320**, 365–369.

Yanagita, M., Oka, M., Watabe, T., Iguchi, H., Niida, A., Takahashi, S., Akiyama, T., Miyazono, K., Yanagisawa, M. & Sakurai, T. 2004. USAG-1: a bone morphogenetic protein antagonist abundantly expressed in the kidney. *Biochem. Biophys. Res. Commun.* **316**, 490–500.

Zhou, H. D., Bu, Y. H., Peng, Y. Q., Xie, H., Wang, M., Yuan, L. Q., Jiang, Y., Li, D., Wei, Q. Y., He, Y. L., Xiao, T., Ni, J. D. & Liao, E. Y. 2007. Cellular and molecular responses in progressive pseudorheumatoid dysplasia articular cartilage associated with compound heterozygous WISP3 gene mutation. *J. Mol. Med.* **85**, 985–996.

Zilberberg, A., Yaniv, A. & Gazit, A. 2004. The low density lipoprotein receptor-1, LRP1, interacts with the human frizzled-1 (HFz1) and down-regulates the canonical Wnt signaling pathway. *J. Biol. Chem.* **279**, 17535–17542.

Differentiation of Bone Marrow Stromal Cells into Osteoblasts in a Self-assembling Peptide Hydrogel: *In* Vitro and In Vivo Studies

MAHO OZEKI,[1] SHINJI KURODA,[1,*] KAZUHIRO KON[1] AND SHOHEI KASUGAI[1,2]

[1]Oral Implantology and Regenerative Dental Medicine
Graduate School, Tokyo Medical and Dental University
1-5-45 Yushima, Bunkyo-ku, Tokyo 113-8549, Japan

[2]Global Center of Excellence (GCOE) Program, International Research
Center for Molecular Science in Tooth and Bone Diseases
Tokyo Medical and Dental University, Tokyo, Japan

ABSTRACT: A prerequisite of tissue engineering approaches with regard to autograft is a suitable scaffold that can harbor cells and signals. Conventionally, such scaffolds have been prepared as 3D scaffolds prefabricated from synthetic or natural biomaterials. RAD16 has been introduced as a new biomaterial, where synthetic peptides self-assemble to form a hydrogel. In this study, RAD16 was examined in terms of osteogenic efficacy and feasibility of ectopic mineralization.

Two hundreds 71 of RAD16 was cocultured with 1×10^6 bone marrow cells from
1 the femurs of 6-week-old Wistar male rats in alpha minimum essential medium supplemented with or without dexamethasone. Second, the same volume of the RAD16 construct hosting the cells with or without hydroxyapatite (HA) particles was treated in the dexamethasone medium as well, prepared in a Teflon tube, and implanted subcutaneously. Cell proliferation was prominent in the RAD16 coculture with dexamethasone at 1 week and significantly decreased by 2 weeks, whereas the other combinations remained or inclined, and their osteogenic differentiation was accelerated up to 2 weeks, as seen in increasing alkaline phosphatase (ALP) activity and mRNAs of ALP, OPN, and OCN. The RAD16 implant prepared with HA particles allowed more osteoblast-like cells and blood

*Author to whom correspondence should be addressed. E-mail: skuroda.mfc@tmd.ac.jp
Figures 1,2,5 and 6 appear in color online: http://jba.sagepub.com

0885-3282/09/00 0001–22 $10.00/0 DOI: 10.1177/0885328209356328

+ [Ver: 8.07r/W] [23.11.2009–5:34pm] [1–22] [Page No. 1] FIRST PROOFS {SAGE_FPP}JBA/JBA356328.3d (jba) Paper: JBA356328 Keyword

cells to grow inside, which was accompanied by elevating OPN gene expression and the stronger peak of VEGF gene expression at 2 weeks. Furthermore, more OPN mRNA signal was detected around the RAD16 containing HA particles by 4 weeks. On the other hand, the RAD16 alone represented lower expression of OPN gene. During the experiment, however, no ectopic mineralization was observed in both groups. Conclusively, it was suggested that the RAD16 showed feasibility of serving as a matrix for osteogenic differentiation of cocultured bone marrow cells in vitro and in vivo. Proceeding of exploration and modification of RAD16 is continuously required for cell-based tissue engineering. 2

KEY WORDS: self-assemble, hydrogel, tissue engineering, RAD16, osteogenesis.

INTRODUCTION

Autologous bone grafts (grafts taken from the same individual in whom they are reimplanted) are still considered the 'gold standard' for reconstruction of compromised bones because of the absence of immunological rejection and the presence of stem cells and growth factors having osteoinductive and osteoconductive properties [1]. However, autologous bone grafting still poses a variety of problems, including donor site morbidity. The limited amount of available bone suitable for harvesting and grafting must be taken into account when autologous bone grafts are considered. Therefore, development of alternatives is clearly a high priority. Allografts (grafts from human cadavers) and xenografts (grafts from animals, typically pigs and cows) have inherent risks and disadvantages, such as the transmission of disease from the donor to the recipient or immunogenic responses. Synthetic bone substitute materials, such as calcium phosphate ceramics, have been used; however, the ceramics are not usually osteogenic.

An alternative approach would be to apply a cell-based strategy, whereby mesenchymal stem cells (MSCs) from bone marrow, for instance, could be grown. Such cultures would have potential for tissue-engineered cartilage and bone repair [2–5]. Although the number of MSCs in bone marrow is relatively small, their numbers can be increased in vitro while maintaining their ability to differentiate into multiple cell lineages. Osteogenic cells can be isolated from bone marrow and induced to grow by an established method [6]. The capacity of MSCs to proliferate and differentiate makes them ideal candidates for bone tissue engineering.

A prerequisite of a tissue engineering approach is a suitable scaffold with an architectural design that is feasible for use in bone tissue engineering applications. Typically, such scaffolds have been prepared ex vivo as 3D structures prefabricated from synthetic or natural

+ [Ver: 8.07r/W] [23.11.2009-5:35pm] [1-22] [Page No. 2] FIRST PROOFS {SAGE_FF}JBA\JBA 356328.3d (jba) Paper: JBA 356328 Keyword

biomaterials [1,7–10]. And these materials and their internal structures have been examined and improved at both micro and nano scales, for instance by electrospinning or phase separation techniques so that they can provide more favorable environment for cell survival and bone regeneration. A new class of biomaterials, synthetic self-assembling peptide-based hydrogel, was initially introduced by Zhang et al. [11] This self-assembling peptide, named EAK16, includes a double unit of (Ala-Glu-Ala-Glu-Ala-Lys-Ala-Lys)$_2$ amino acid residues and has a characteristic b-sheet circular dichroic spectrum in water, with minimum and maximum ellipticities at 218 and 195 nm, respectively [12,13]. EAK16 comprises self-complementary amphiphilic oligopeptide pairs of positively charged lysine- and negatively charged glutamic acid side chains on one side and hydrophobic alanine side chains on the other side. Self-complementary EAK16 is distinctive from many synthetic peptides in that it forms an insoluble macroscopic membrane; when the peptide solution is exposed to a physiological medium or salt solution, it rapidly forms nanometer-scale fibers and assembles into 3D hydrogel scaffolds. Another version of EAK16, RAD16, was also constituted by Zhang et al. [14]. In RAD16, positively charged arginines substitute for lysines and negatively charged aspartic acids substitute for glutamic acids. Previous studies have reported cell attachment and differentiation when supported by those carriers [14–19] as well as the bone formation potential of bone marrow cells (BMCs) combined with the hydrogel scaffolds [9,20,21]. In addition, these hydrogels have been shown to repair critical-sized bone defects; however, few reports have compared these hydrogel scaffolds with conventional biomaterials with regard to bone formation [21].

The present study consisted of both *in* vitro and in vivo experiments: The *in* vitro study examined the osteogenic efficacy of PuraMatrix™ (3-DMatrix Japan, Tokyo, Japan), a hydrogel of RAD16, on rat BMCs cultured with or without a set of osteogenic supplements. The hydrogel complexes were then implanted subcutaneously into rats in the in vivo study and analyzed for mineral apposition in the matrix. Simultaneously, we also investigated ectopic bone formation ability using a combination of RAD16 harboring the BMCs and hydroxyapatite (HA) particles capable of regenerating bone [22–26].

MATERIALS AND METHODS

The animal experiments in this study were performed under the 'Guidelines for Animal experimentation' of Tokyo Dental and Medical University, Tokyo, Japan. The animal welfare committee of Tokyo

+ [Ver: 8.0.r/W [23.11.2009-5:35pm] [1-22] [Page No. 3] HIST PROOFS (SICE_HP_JBM_JBA_36328.3d (jba) Paper: JBA_36328 Keyword

Dental and Medical University approved the experimental procedures regarding use and care of animals.

Biomaterials

PuraMatrix™ was kindly donated by 3-DMatrix Japan. The synthesis and characterization of RAD16 has been described previously [14]. RAD16 has the amino acid sequence AcNRADARADARADARADA-CNH2 (in single letter amino acid code) and is soluble in salt-free aqueous solutions. When RAD16 is exposed to a solution containing salt, such as physiological medium including saline, the peptide self-assembles spontaneously form hydrogel-producing nanofibers within the gel, which has a water content of over 99%. Yokoi et al. described the hydrogel-forming mechanism and physical properties of the formed hydrogel in more detail [25]. The sterilized RAD16 solution was provided in vials at a peptide concentration of 10 mg/mL.

Animals

Six- and ten-week-old male Wistar rats (Sankyo Lab. Inc., Tokyo, Japan) were used. The rats were kept in standard rat cages with free access to dry pellets and water with unrestricted movement at all times during feeding. All surgical procedures on the animals were performed under general anesthesia by intraperitoneal injection of sodium pentobarbital (body weight, 40 mg/kg; DS Pharma Biomedical Co., Ltd., Osaka, Japan).

Preparation of Rat BMCs

BMCs were obtained from the femoral medulla of 6-week-old Wistar male rats after sacrifice and prepared as follows (Figure 1).

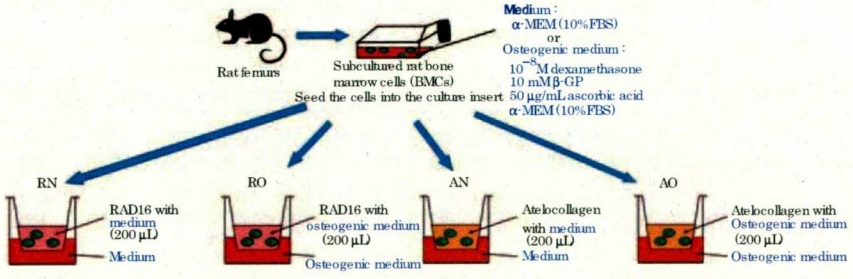

Figure 1. Scheme of the preparation of the four different constructs for the cell culture.

+ [Ver: 8.0r/W [23.11.2009-5:35pm] [1-22] [Page No. 4] HIST PROOFS {SCE_HP}JBA356383d (jba) Paper: JBA356383 Keyword

Both proximal and distal ends of the femurs were cut away from the epiphysis, and the marrow was flushed out using 10 mL of alpha minimum essential medium (aMEM; Invitrogen, Burlington, ON, Canada) expelled from a syringe through a 21-gauge needle. The released cells were collected in a 175-mL flask (BD Biosciences, Bedford, MA, USA) containing 20 mL of the aMEM supplemented with 10% fetal bovine serum (FBS; JRH Biosciences, Lenexa, KS, USA) and antibiotics (100 U/mL penicillin: Invitrogen; 0.25 mg/mL amphotericin B: Sigma Chemical, St. Louis, MO, USA). In order to remove nonadherent cells, the medium was changed after 24 h. Subconfluent cells in the primary culture were harvested after treatment with 0.25% trypsin/0.05 mmol EDTA solution (Sigma Chemical) and were subcultured in the culture medium, aMEM (10% FBS). The medium used was with or without the following osteogenic reagents: 10 nmol dexamethasone (Dex; ICN Pharmaceutical, Irvine, CA, USA), 10 mmol b-glycerophosphate (b-GP; EMD Biosciences, San Diego, CA, USA), and 50 mg/mL ascorbic acid (Vc; Sigma-Aldrich, St. Louis, MO, USA). During the culture period, cells were incubated at 378C in a humidified atmosphere of 5% CO_2 with medium replacement every 3 or 4 days, and reseeded into the flasks when they became confluent.

BMC Encapsulation

Figure 1 shows the process used for the preparation of the different constructs. After several passages of the culture, the BMCs incubated in both ways (with or without the osteogenic supplements) were trypsinized and encapsulated in the RAD16 hydrogel according to the manufacturer's instructions. After washing with aMEM, 100 mL of a 10% sucrose suspension of 1×10^6 cells with or without osteogenic supplements (corresponding to each culture condition) was combined with the same volume of the 1% RAD16 hydrogel. Subsequently, the entire 200 mL mixture was transferred into cell culture inserts in a 24-well cell culture plate. To form the hydrogel to encapsulate the MSCs, 500 mL of each culture medium was added to the lower chambers of the inserts by pipetting down the side of the outer well between the cell culture insert and the 24-well cell culture plate before the 200 mL cell suspension mixture was transferred into each cell culture insert. To prevent drying of the formed hydrogel surface, each culture medium was carefully layered onto the hydrogel by running it slowly down the inner wall of the insert. During the following 30 min, the medium in the culture plate (but outside the insert) was changed twice to equilibrate the growth environment to physiological pH and then incubated for 24 h

+ [Ver: 8.0r/W] [23.11.2009-5:35pm] [1-22] [Page No. 5] HIST PROOFS {SICE_HP:JBA:JBA356283.3d (jba)} Paper: JBA_35628 Keyword

in a humidified atmosphere of 95% air and 5% CO_2 at 378C. The BMCs encapsulated within the gel were cultured for 7 and 14 days; the media were changed every 2–3 days.

In Vitro **St**udies

The BMCs/RAD16 constructs were then directly used for ***in*** vitro analyses as the RO group for RAD16 in the osteogenic media and the RN group for RAD16 in the normal media. The same number of cultured BMCs with or without the osteogenic supplements were also mixed in 200 mL of 0.24% atelocollagen gel to form two sets of atelocollagen matrices; that is, the AO group for atelocollagen in the osteogenic media and the AN group for atelocollagen in the normal media. The number of samples in each group was four or five for each analysis per time point.

In Vivo **St**udies

For the animal study, implant composites harboring the MSCs in the osteogenic environment only were similarly prepared in Teflon tubes 7 mm in diameter and 3 mm in height, positioned in the center of the inside bottom of the insert during the gel-making process that produced the RAD16 group. Prior to the main animal study, a preliminary study was briefly performed that RAD16 was implanted subcutaneously in the rat without cocultured cells for an analysis of its degradation and contraction and that the sample retrieved from the animal showed slight contraction of RAD16 even after 24 h. Therefore, a skeleton was required to keep the implant volume just for the animal study. HA has been widely recognized as a promising bone substitute, a space keeper, and a bone conductor in orthopedic and dental fields. Then, another version of the implant that included HA particles was additionally prepared as the RAD16 + HA group to expect more potential for osteogenesis than RAD16 alone. The HA particles used in the present study were kindly provided with their size of 500–700 mm in diameter to keep the space of RAD16 and with interconnecting pores of 100 mm to allow surrounding cells to invade and angiogenesis to expand in the particles by Advance Co. Ltd., Tokyo, Japan. The HA particles were mixed without homogenization during the self-assembling at a concentration of 5% (w/w) and 5% (v/v) and did not affect the process of the gel formation. The composites in the Teflon tubes were then used as the implants in the animals. Twelve Wistar rats were used. Six were implanted with RAD16 structures and six with RAD16 + HA structures. Within each group of six, half were used for RNA expression analysis and half for histological and

+ [Ver: 8.07r/W] [23.11.2009–5:35pm] [1–22] [Page No. 6] FIRST PROOFS {SAGE_FTP}JBA/JBA356328.3d (jba) Paper: JBA356328 Keyword

immunochemical analysis. Quartets of rats were sacrificed at 1, 2, and 4 weeks. At each sacrifice, four rats were available for evaluation: RAD16 for RNA expression, RAD16 + HA for mRNA expression, RAD16 for histology and immunology, and RAD16 + HA for histology and immunology.

DNA Amount and Alkaline Phosphatase Activity

A set of cultured BMCs in the hydrogel was centrifuged, washed with phosphate-buffered solution (PBS), lysed by 0.1% Triton (Sigma Chemical), and sonicated to destroy cell membranes. After centrifugation (15,000 rpm, 10 min at 48C), 100 mL of the supernatant was extracted from each sample and assayed for DNA content and alkaline phosphatase (ALP) activity. To determine DNA content, 10 mL of the prepared supernatant of each sample was mixed with 200 mL of 2 mg/mL Hoechst 33258 dye in a well of a 96-well plate and processed with a fluorescent DNA quantitation kit (Bio-Rad Laboratories, Hercules, CA, USA). The samples were then measured with the Wallac 1420 ARVOsx multilabel counter at emission and excitation wavelengths of 365 and 460 nm, respectively. Subsequently, 20 mL of the supernatant of each sample was used for quantitative and kinetic determination of ALP activity by adding it to the 100 mL working solution (r-nitrophenylphosphate solution) in a well of another 96-well plate. The colorimetric measurement was performed with the multilabel counter at a wavelength of 405 nm. ALP activity was normalized by total DNA amount at each time point.

RNA Isolation and Real-time Quantitative Real-time Polymerase Chain Reaction

BMCs from both the culture and the animal studies were subjected for a gene expression analysis. They were centrifuged and washed with PBS as well, but lysed in TRIzol® solution (Life Technologies, Burlington, ON, Canada) for total RNA extraction. After the total RNA was precipitated in isopropanol, the first-strand cDNA was reverse-transcribed from the total RNA with SuperScript™ III First-Strand Synthesis Super Mix (Invitrogen). All cDNAs were subjected to the polymerase chain reaction (PCR) for glyceraldehyde 3-phosphate dehydrogenase (GAPDH) mRNA as a test of RNA integrity and cDNA synthesis. Subsequently, equal volumes of cDNA were used to program a quantitative analysis for osteoblast-related genes, such as collagen I (COL I), ALP, osteopontin (OPN), osteocalcin (OCN), vascular

endothelial growth factor (VEGF), and GAPDH as a housekeeping gene. The gene expression of interest was determined by a real-time PCR (RT-PCR). Amplification primer sets used are listed in Table 1. SYBR green (dye)-based RT-PCR analysis was carried out with the ABI Prism 7300 Sequence Detection System (Applied Biosystems, Foster City, CA, USA). Expression levels of the genes examined were normalized by that of GAPDH within the same sample. A conventional RT-PCR was also performed under the following condition: Up to 42 cycles of denaturing at 948C for 30 s, annealing at 608C for 30 s, and extension at 728C for 30 s with a final extension at 508C for 10 min. The PCR products were run in 2.0% (w/v) agarose gel by electrophoresis and visualized by ethidium bromide staining.

Implantation into Rats

As described earlier, for the in vivo assay for osteogenesis, 12 10-week-old male Wistar rats were used. Under general anesthesia (intraperitoneal injection of 100 and 8 mg/kg body weight of ketamine and xylazine, respectively), the backs of rats were shaved and disinfected with povidone iodine (Isodine; Meiji Seika Kaisha, Tokyo, Japan). The dorsal skin of the animals was incised close to the scapula on both sides across the vertebra at right angles, and then subcutaneous pockets were prepared in each rat. Each rat received four identical implants of its assigned composite in individual subcutaneous pockets alongside the

Table 1. Description of the designed primers and probes.

Gene	Forward and reverse primers	Fragment length (bp)
rCOL I	5′-ttg acc cta acc aag gat gc 3′-cac ccc ttc tgc gtt gta tt	197
rALP	5′-gtc aca gcc agt ccc tca ac 3′-tat tcc aaa cag ggg agt cg	201
rOPN	5′-ttt ccc tgt ttc tga tga aca gta t 3′-ctc tgc tta tac tcc ttg gac tgc t	200
rOCN	5′-agc tca acc cca att gtg ac 3′-agc tgt gcc gtc cat act tt	190
rCOL II	5′-gta cac tgc cct gaa gga tg 3′-att gtg ttg ttt tgg ggt tg	201
rVEGF	5′-ttg aga ccc tgg tgg aca tc 3′-ctc cta tgt gct ggc ttt gg	192
rGAPDH	5′-aac tcc cat tct tcc acc tt 3′-gag ggc ctc tct ctt gct ct	200

vertebra: Six rats received four RAD16 structures each and six received RAD16+HA structures. The incised wounds were then sutured. The animals were euthanized by intraperitoneal injection of an excessive dose of sodium pentobarbital at 1, 2, and 4 weeks, and the specimens were subjected to histology and total RNA extraction analyses.

Histological Sections

The sacrificed specimens were immediately fixed in 10% neutral formalin buffer solution (Wako, Osaka, Japan) for approximately 24 h at 48C, followed by decalcification process in 10% EDTA, pH 6.3, for 14 days at 48C. The samples were then washed with diethyl pyrocarbonate; dehydrated in a graded series of ethanol (70–100%); and embedded in paraffin (melting point, 56–588C). Histological sections 5 mm in thickness were cut and transferred onto 3-aminopropyrytrietoxy silane-coated glass slides. Each section was stained with hematoxylin and eosin.

In Situ Hybridization

RNA probes for rat osteocalcin (175 bp) and rat osteopontin (200 bp) mRNA were prepared by transcribing cDNAs of the appropriate genes inserted into vectors using the following protocol: cDNAs as PCR products were amplified using RT-PCR with their specific oligonucleotide primer sets designed by Primer3 (v. 0.4.0) software (Whitehead Institute for Biomedical Research, Cambridge, MA, USA) (Table 1). In addition, the PCR products were cloned into pCRII®-TOPO® vectors and amplified in TOP10F′ Escherichia coli, and the plasmid DNAs were isolated and purified with an EndoFree Plasmid Maxi Kit (Qiagen). Both sense and antisense digoxigenin-11-UTP-labeled single-strand RNA probes were synthesized with SP6/T7 RNA polymerases prepared using a digoxigenin (DIG) RNA labeling kit (Roche Diagnostics GmbH, Mannheim, Germany). In situ hybridization for the detection of osteocalcin and osteopontin expression proceeded as follows: In each hybridization experiment, two sets of sections from the same sample were hybridized separately with the antisense and sense riboprobes under identical experimental conditions. In situ hybridization was performed with commercial in situ hybridization reagents (Nippon Gene, Tokyo, Japan). Hybridization was performed for 16 h at 428C. After DIG-labeled probes were detected with a commercial nucleic acid detection kit (Roche Diagnostics), each section was stained with methyl green and mounted with Mount-Quick™ mounting medium (SPI Supplies and Structure Probe, Inc., West Chester, PA, USA).

+ [Va: 807r/W] [2311.2009-535pm] [1-22] [Page No 9] HIST PROOFS {SCE_HP_BA_BA356283d} (jha) Paper: JBA356328 Keyword

Statistical Analyses

Statistical analyses were performed with the statistical software package, SPSS 14.0 for Windows (SPSS Inc., Chicago, IL, USA). Data were analyzed with the nonparametric Kruskal-Wallis test, followed by Mann–Whitney tests for two-group comparisons. Data were considered statistically significant when a p-value was equal to or less than 0.05. Results are expressed as mean values ± standard deviation (SD).

RESULTS

The Hydrogels after Incubation

The atelocollagen gel form contracted only when incubated in aMEM without dexamethasone (AN group) for 2 days; on the other hand, the atelocollagen cocultured in the dexamethasone medium (AO group) and the two groups of RAD16 (RN and RO groups) maintained their volumes over the period (Figure 2).

In Vitro Studies

CELL PROLIFERATION IN RAD16 HYDROGEL AND ATELOCOLLAGEN

Levels of cellular DNA were assessed as a measure of cell number for each of the material types investigated in this study (Figure 3(A)). Cell proliferation proceeded significantly in the RAD16 hydrogel treated with the osteogenic medium (RO group) compared with that in the RAD16 with aMEM (RN group) and with that in the atelocollagen with the osteogenic medium (AO group) at 1 week. Although the averaged DNA amount of the RO group was the largest, it had no significance when compared with that of the AN group, which indicated a larger DNA

Figure 2. The hydrogels after incubation. Contraction of the hydrogel occurred only in the AN group. No contraction was observed in the RO, RN, and AO groups.

+ [Ver: 8.07r/W] [23.11.2009-5:35pm] [1-22] [Page No. 10] FIRST PROOFS {SAGE_FTP}JBA/JBA 356328.3d (jba) Paper: JBA356328 Keyword

amount than the RN group. Subsequently, the concentration of DNA in the RO group decreased significantly by week 2, and the other groups showed increased or no change in DNA amount.

ALP BIOACTIVITY

The ALP activity of the cells in the constructs was expressed and normalized by their DNA quantities (Figure 3(B)). The lowest ALP activity of the RO group at week 1 increased drastically by week 2 to become the highest. On the other hand, ALP activity in groups RN and AO did not change significantly, and ALP activity in the AN group declined prominently.

OSTEOBLASTIC GENE EXPRESSION IN CULTURE

As shown in Figure 4, gene expressions of interest in the cultured cells were evaluated at different time points. The two kinds of RAD16 composites (RO and RN) expressed the OPN gene higher than the atelocollagen constructs over the 2-week period (Figure 4(A)); OPN gene expression of the RO group dramatically increased over the 2-week period. Although the AO group also showed increased OPN gene expression, it did not reach the level of the RO group. OCN gene expression was less detected at 1 week but surprisingly upregulated at 2 weeks in the two osteogenic treatment groups (RO and AO groups) (Figure 4(B)). Interestingly, although OCN gene expression was observed to be less in the atelocollagen matrix treated with aMEM, the RAD16

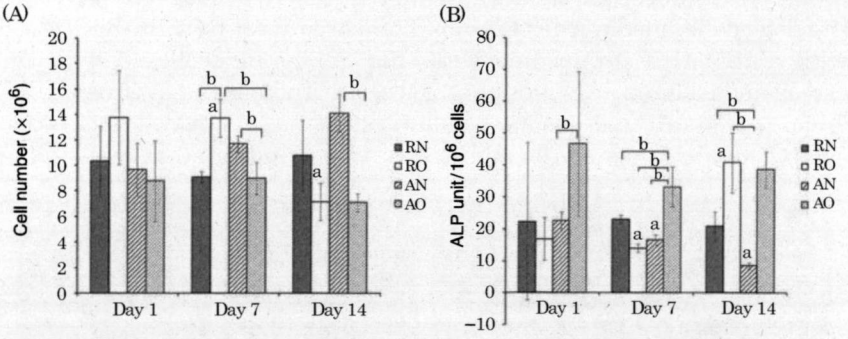

Figure 3. Cell growth and ALP activity *in* vitro. (A) Cell number was measured to evaluate the cell growth. (B) A quantitative analysis of ALP activity was measured by normalizing the total ALP amount by cell number. The results are expressed as ALP unit/106 cells. Experiment values were each expressed as the mean ± SD (n = 6). a: Statistically significant difference compared in the same group (p5 0.05). b: Statistically significant difference compared to all other groups (p5 0.05).

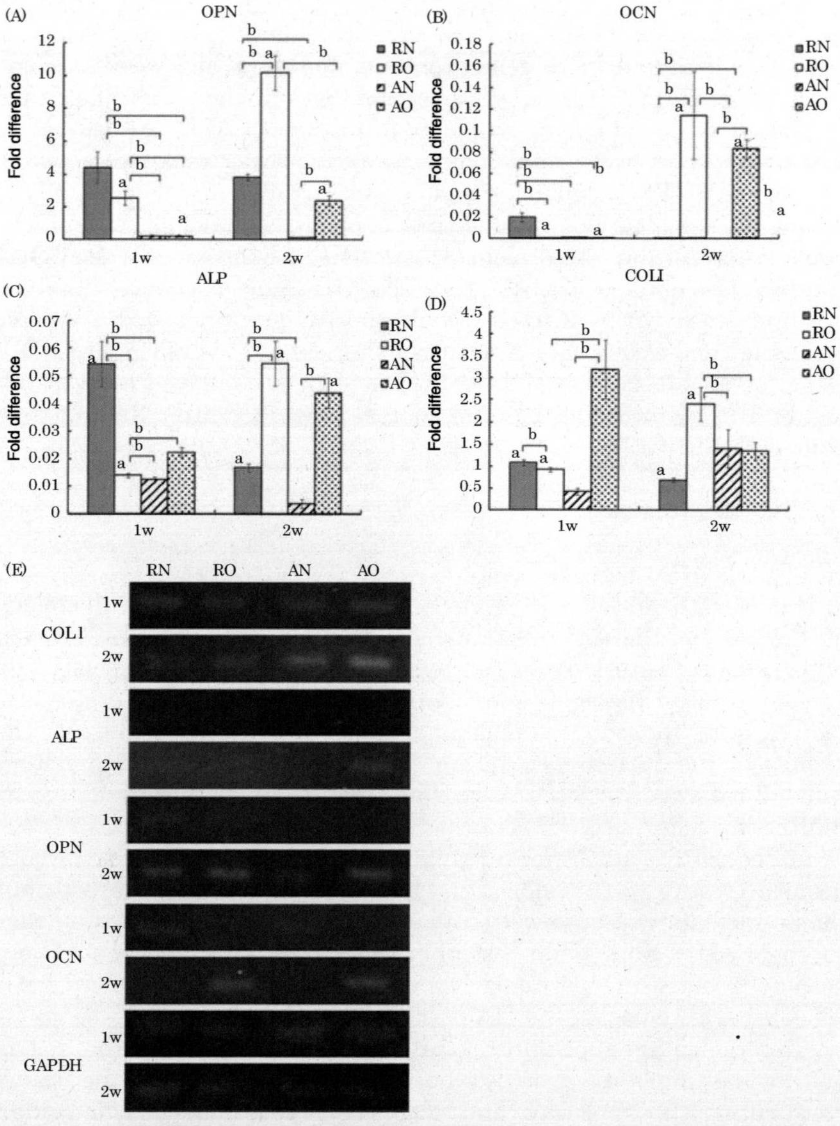

Figure 4. Osteogenic gene expression in culture. Representative curves of mRNA expression levels of OPN (A), OCN (B), ALP (C), and COL I (D) in each group are calculated by the 2::Ct formula. Experiment values are each expressed as the mean ± SD (n = 3). a: Statistically significant difference compared in the same group (p5 **0.05**). b: Statistically significant difference compared to all other groups (p5 0.05). Gel electrophoresis (E) showed different gene expression levels corresponding to the quantitative analysis at different time points.

matrix cultured in aMEM showed significant OCN gene expression at 1 week. Subsequently, the gene expression faded out at 2 weeks. On the other hand, the OCN gene was expressed less in the atelocollagen gel incubated in aMEM during this period. In terms of ALP, the osteogenic treatment groups were well stimulated during the 2-week period, while the normal aMEM incubated matrices were significantly downregulated during the same period, representing an opposite tendency between the two different medium treatments (Figure 4(C)). Expression of the COL I gene was also notable: The AO group showed strong expression at 1 week but dropped down by 2 weeks, while the RO group showed a weaker expression at 1 week but significantly increased at 2 weeks (Figure 4(D)). Gel electrophoresis showed different gene expression levels corresponding to the quantitative results by real-time PCR at different time points (Figure 4(E)).

In Vivo Studies

HISTOLOGICAL FINDINGS

The RAD16 and RAD16+HA groups presented similar histology at 1 week but the findings gradually diverged over time. At 1 week, both samples were surrounded by gathering inflammatory cells and generated blood vessels (Figure 5(A) and (B)). There were residual gel pieces in the two groups, and giant cells were seen to permeate into the sample of the RAD16+HA group in advance of other inflammatory cells. Furthermore, the HA residues began to be encapsulated by infiltrating cells.

Subsequently, at 2 weeks, inflammatory cells increased in both groups (Figure 5(C) and (D)). RAD16 was being absorbed but maintained its presence better in the RAD16+HA group. Contrary to the RAD16 absorption, osteoblast-like cells and blood cells were seen to be increasing; particularly, the RAD16+HA group allowed those cells to begin replacing the HA particles.

After remaining subcutaneous for 4 weeks, not only did the matrix gel in the implants decrease but the total volume of the tissue constituting the implanted and endogenous cells also shrank to half the original volume in the RAD16 group (Figure 5(E)), whereas the RAD16+HA group continued to retain the tissue filling the inside of the Teflon tube (Figure 5(F)). Although the HA particles were viewed to be a little absorbed by permeating cells, the final volume of the HA particles did not change so much from the initial volume of 5% (v/v) and 5% (w/w). Notably, more blood vessels were observed in the RAD16+HA group.

+ [Ver: 8.0.7r/W] [23.11.2009-5:35pm] [1-22] [Page No. 13] HISTROIS {SCE_HP_JBA_36328d} (jba) Paper: JBA_36328 Keyword

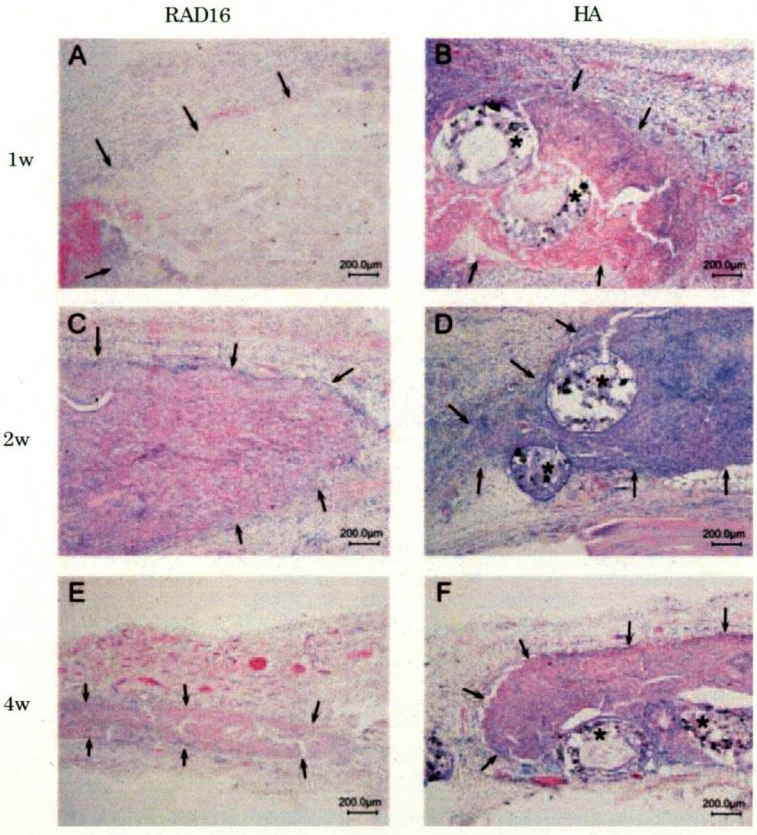

Figure 5. Histology of the implanted hydrogels. The specimens harvested from the subcutaneous pockets were stained with hematoxylin and eosin. The RAD 16 hydrogel of both the RAD 16 (A, C, E) and the HA (B, D, F) groups remained till the 4 weeks period. 'Arrows' indicate the hydrogel area and 'asterisks' indicate hydroxyapatite particles. Magnification: ×16. Bar: 200 mm.

LOCALIZATION OF OSTEOPONTIN AND OSTEOCALCIN mRNAs

The localization of two osteogenesis-related genes was examined on the paraffin sections (Figure 6). Osteopontin was observed inside and evenly along the rim of the grafted materials with a weak signal strength at 2 weeks, although it was not detected at 1 week in either group. The signal was restricted along the rim at 4 weeks (Figure 6(C)). This signal was expressed somewhat more strongly in the RAD16 + HA group than in the RAD16 group over the period. The signal of the other gene, osteocalcin, was weaker than that of osteopontin during the experimental period, but it was distributed in a similar pattern to osteopontin (Figure 6(E) and (G)).

+ [Ver: 8.07r/W] [23.11.2009-5:35pm] [1-22] [Page No. 14] [FIRST PROOFS] {SCE_EP_JBA_356383d} (jba) Paper: JBA_35638 Keyword

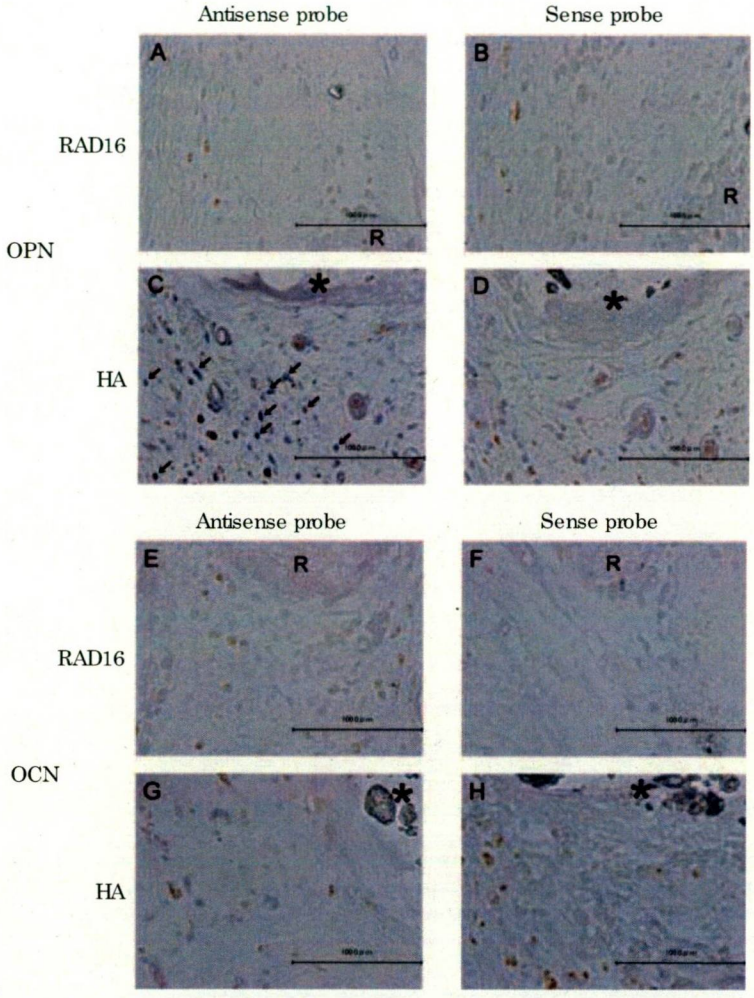

Figure 6. In situ hybridization. In situ hybridization on the sections using DIG-labeled antisense probes for mRNA of rat osteopontin at 4 weeks. The specimen of HA group (C) represents mRNA expression of osteopontin (arrows) localized inside and along the rim of the grafted materials. 'Asterisks' indicate hydroxyapatite particles and 'R' indicates the RAD 16 hydrogel area. Magnification: ×800. Bar: 100 mm. No signal of rat osteocalcin gene was observed (data not shown).

GENE EXPRESSIONS IN THE GRAFTED RAD16s

The osteogenesis-related genes, which were examined in the culture study, were assayed by PCR analysis together with the VEGF gene (Figure 7). The expression of COL1, ALP, and VEGF genes demonstrated

+ [Ver: 8.07r/W] [23.11.2009-5:35pm] [1-22] [Page No. 15] HIST PROOFS {SICE_FP}JBA/JBA356283.3d (jba) Paper: JBA_35628 Keyword